

United States  
Department of  
Agriculture

Natural Resources  
Conservation  
Service

11 Campus Boulevard  
Suite 200  
Newtown Square, PA 19073

**Subject:** Eng – Electromagnetic Induction (EMI) Field Assistance

**Date:** 22 November 2000

**To:** Patricia S. Leavenworth  
State Conservationist  
6515 Watts Road, Suite 200  
Madison, Wisconsin 53719-2726

**Purpose:**

An EMI survey was conducted at Site Number 24, Bad Axe Watershed to gather information on the nature of a partial breach along the left abutment.

**Participants:**

Bruce Brown, Wisconsin Geological and Natural History Survey, Madison, WI  
Ritchie Brown, Division Manager, Ho-Chunk Nation, DNR, Black River Falls, WI  
Dan Chroninger, Technician, Vernon County LCD, Viroqua, WI  
Jim Doolittle, Research Soil Scientist, USDA-NRCS, Newtown Square, PA  
Phil Hahn, Resource Conservationists, Vernon County LCD, Viroqua, WI  
Adam LeGarde, Ho-Chunk Nation, DNR, Black River Falls, WI  
Barbara Lensch, Geologist, USDA-NRCS, Madison, WI  
Scott Mueller, Agricultural Engineer, USDA-NRCS, Dodgeville, WI  
Dan Reid, Wisconsin Geological and Natural History Survey, Madison, WI  
Rex Whitegull, Ho-Chunk Nation, DNR, Black River Falls, WI

**Activities:**

All activities were completed on 9 November 2000.

**Background:**

Site 24, Bad Axe Watershed is located in the southwest quarter of Section 29, T12N, and R5W in Vernon County, Wisconsin. The site is located about eight miles southwest of the town of Viroqua. The structure was completed in August 1967. The embankment is about 39 feet high and 320 ft long.

Following a severe rainfall event (May 31 to June 1, 2000), slumping and several holes were discovered along both the upstream and downstream portions of the left abutment. The holes were small and less than a few feet in diameter. Near the downstream hole, a debris trail was observed that extended to the creek below the plunge pool. After another rainfall event on 14 June 2000, water was observed flowing into holes on the upstream side of the left abutment. However, no water was observed flowing from the hole located on the downstream side of the left abutment.

Site 24 is underlain by sandstone bedrock. The Van Oser member of the Jordan Formation outcrops in the slump area along the upstream side of the left abutment. The Norwalk member of the Jordan Formation outcrops near the "exit" hole along the downstream side of the left abutment. Both members consist of jointed bedrock.

**Equipment:**

The GEM300 sensor, developed by Geophysical Survey Systems, Inc.,<sup>1</sup> was used in this study. This sensor is configured to simultaneously measure up to 16 frequencies between 330 and 19,950 Hz with a fixed coil separation (1.3 m). Won and others (1996) have described the use and operation of this sensor. The theoretical penetration

<sup>1</sup> Trade names are used to provide specific information. Their mention does not constitute endorsement by USDA- NRCS

depth of the GEM300 sensor is dependent upon the bulk conductivity of the profiled earthen material(s) and the operating frequency. With the GEM300 sensor, the depth of penetration is considered "skin depth limited". The skin-depth represents the maximum depth of penetration and is frequency and soil dependent: low frequency signals travel farther through conductive mediums than high frequency signal. Multifrequency sounding with the GEM300 allows multiple depths to be profiled with one pass of the sensor.

To help summarize the results of this study, the SURFER for Windows program, developed by Golden Software, Inc.,<sup>2</sup> was used to construct two- and three-dimensional simulations of the study site. Grids were created using kriging methods with an octant search.

### **Field Procedures:**

A 330 by 270 foot rectangular grid was established across the structure and adjoining abutments. Ten survey lines were established across the study site at intervals of 30 feet. These lines paralleled the centerline of the structure. One hundred and eight survey flags were inserted in the ground at intervals of 30 feet along the ten survey lines and served as survey points (see Figure 1). At each survey point, the elevation of the ground surface was determined with a total station instrument.

The GEM300 sensor was operated in both the continuous and station modes. In the continuous mode, the GEM300 sensor was configured to record an observation every two seconds. Measurements were taken with the GEM300 sensor held at hip-height in the vertical dipole orientation. At each observation point, in-phase, quadrature phase, and conductivity data were recorded at four different frequencies (3030, 6150, 9810, and 14790 Hz). Frequencies of 9810 and 14790 Hz correspond to the operating frequencies of the EM31 and EM38 meters (manufactured by Geonics, Limited<sup>2</sup>), respectively. Walking at a uniform pace along each of the ten parallel survey lines resulted in 584 observations. The locations of these observations were processed and adjusted by the MAGMAP96 software program (developed by Geophex Limited<sup>2</sup>). The locations of these observation points are shown in Figure 2. In the station mode, the GEM300 sensor was manually operated in both horizontal and vertical dipole orientations at each of the survey points shown in Figure 1. This procedure provided 108 observations. At each observation point, in-phase, quadrature phase, and conductivity data were recorded at four different frequencies (3030, 6150, 9810, and 14790 Hz).

### **EMI:**

#### Background:

Electromagnetic induction is a noninvasive geophysical tool that has been used to investigate dam foundations (Butler et al., 1989) and to locate water-bearing fracture zones in bedrock (McNeill, 1991; Olayinka, 1990). Advantages of EMI are its portability, speed of operation, flexible observation depths, and moderate resolution of subsurface features. Results of EMI surveys are interpretable in the field. This geophysical method can provide in a relatively short time the large number of observations needed to comprehensively cover sites. Maps prepared from correctly interpreted EMI data provide a means for assessing site conditions, planning further investigations, and locating sampling or monitoring sites.

Electromagnetic induction measures vertical and lateral variations in magnetic and/or electrical fields associated with induced subsurface currents. Data are expressed as in-phase, quadrature phase, or apparent conductivity. In-phase refers to the part of the signal that is in phase (has zero phase shift) with the primary or reference signal. The in-phase signal is sensitive to buried metallic objects and has been referred to as the "metal detection" mode.

Quadrature phase refers to the part of the signal that is 90 degrees out of phase with the primary signal. The quadrature phase response is linearly related to the ground conductivity. Some highly conductive targets with small cross-sections, such as pipes, may show up better in the quadrature phase because of the channelization of current. With the GEM300 sensor, in-phase and quadrature phase data are expressed in parts per million (ppm).

Traditionally, EMI data are expressed as apparent conductivity. The GEM300 sensor automatically converts data recorded in the quadrature phase into apparent conductivity. Values of apparent conductivity are expressed in

<sup>2</sup> Trade names are used to provide specific information. Their mention does not constitute endorsement by USDA- NRCS

milliSiemens per meter (mS/m). Apparent conductivity is a weighted, average conductivity measurement for a column of earthen materials to a specific depth (Greenhouse and Slaine, 1983). Variations in apparent conductivity are produced by changes in the electrical conductivity of earthen materials. The electrical conductivity of soils is influenced by the volumetric water content, type and concentration of ions in solution, amount and type of clays in the soil matrix, and temperature and phase of the soil water (McNeill, 1980). The apparent conductivity of soils increases with increased soluble salts, water, and clay contents (Kachanoski et al., 1988; Rhoades et al., 1976).

Electromagnetic induction measures vertical and lateral variations in apparent electrical conductivity. Values of apparent conductivity are seldom diagnostic in themselves, but lateral and vertical variations in these measurements can be used to infer changes in earthen materials. Interpretations are based on the identification of spatial patterns within data sets. To assist interpretations, computer simulations are normally used. Because of their higher moisture and clay contents, it was expected that areas of seepage would have slightly higher apparent conductivity than adjoining areas of the abutment and, if sufficiently large and contrasting, could be detected with EMI.

#### Depth of Observation:

With the GEM300 sensor, the depth of penetration or the “skin depth” is estimated using the following formula (McNeill, 1996):

$$D = 500 / (s \cdot f)^2 \quad [1]$$

Where  $s$  is ground conductivity (mS/m) and  $f$  is frequency (kHz). With the GEM300 sensor held at hip height in the vertical dipole orientation, the average apparent conductivities were 25.2, 18.3, 15.2, and 16.2 mS/m at frequencies of 3030, 6150, 9810, and 14790 Hz, respectively. Based on equation [1], the selected frequencies and these averaged conductivities, the estimated skin depths were about 57 m at 3030 Hz, 47 m at 6150 Hz, 15 m at 9810 Hz, and 16 m at 14790 Hz. Within the defined skin depth, earthen materials from all depths contribute, in varying degrees, to the measured response. Shallow depths contribute more to the measured response than deep layers. While the induced magnetic fields may achieve these estimated skin depths, the strengths of the response diminish with increasing depth and for deeper layers, and are too weak to be sensed by the GEM300 sensor.

The depth of observation is often defined as the depth that contributes the most to the total EMI response measured on the ground surface. Although contributions to the measured response come from all depths, the contribution from the *depth of observation* is the largest (Roy and Apparao, 1971). As noted by Roy and Apparao (1971), for any system, the depth of observation is a good deal shallower than is generally assumed or reported. As no depth-weighting functions are presently available for the GEM300 sensor, it is unclear what depth is providing the maximum response. However, it is clear that the depth of observation is appreciably shallower than the skin depth.

#### **Results:**

Data collected in the continuous mode, vertical dipole orientation, and at frequencies of 3030, 6150, and 9810 Hz are shown in Figure 3. In Figure 3, in-phase and apparent conductivity data are shown in the upper and lower plots, respectively. These image maps use different colors to represent the data. Colors are associated with percentage values (in relation to the minimum and maximum values). In the plots of the in-phase data, the color interval is 10 ppm. In the plots of the conductivity data, the color interval is 1 mS/m. The locations of the flagged, survey points are shown in the upper left-hand plot (3030 Hz, in-phase). The frequency at which data were collected is shown above each plot. The depths of penetration and observation are assumed to increase as the frequency decreases. Spatial patterns shown in each plot reflect the actual measured values, the frequency and unequal distribution of observation sites, and the computer-simulated expression of the data set.

In all plots shown in Figure 3, the two most conspicuous point anomalies represent interference from the inlet (I) and outlet (O) structures of the dam. These anomalies have been labeled in each plot, have rectangular patterns, and have high signal amplitudes (red color). In each plot, three point anomalies (P) are apparent along the lower portion of the upstream embankment. In the in-phase data (upper plots), one additional point anomaly is evident along the downstream side of the left abutment. This anomaly is located near the “exit” hole. Depending on whether the object is ferrous or nonferrous, the anomalous values may manifest themselves as opposite polarities at different

frequencies.

In the plots of in-phase data shown in Figure 3, several structural features are evident. Three linear features have been identified, and highlighted with dark segmented lines. These features occur along survey lines 4, 5, and 7 (measured from the bottom of the plot). The three linear features are best defined in the plot of the in-phase data collected at 3030 Hz. The linear feature along survey line 7 is more contrasting (has higher, positive signal amplitudes (yellow color)) and is evident in all three in-phase plots shown in Figure 3. The linear features along survey line 4 and 5 are less conspicuous (lower, negative amplitude) and most apparent in the data collected at 3030 Hz. These linear features may represent buried foundation drainages that were installed to prevent soil piping and to improve embankment stability. In addition, four conspicuous, high amplitude point anomalies (A and B) occur at each end of the linear features on survey line 4 and 7. These features are presumed to be related to the foundation drainage.

The in-phase data appear to provide information concerning the location of buried structural and cultural features. However, the data provided little to no information concerning the breach in the left abutment. The point anomaly (P) on the downstream side of the left abutment is located near the "exit" hole. While this anomaly is attention grabbing, it may only represent interference from wire fencing. No subsurface conduit for water flow along the left abutment is evident in these plots.

In Figure 3, the plots of apparent conductivity (lower plots) are closely similar. In these plots, lower values are associated with areas having lower clay and/or moisture contents, and shallower depths to resistive sandstone bedrock. Higher values are associated with the wetter, lower-lying pool area, areas of higher clay content and/or deeper depths to bedrock. In the plots of apparent conductivity, the high clay content of the earthen core is responsible for relatively high values (16 to 20 mS/m) of apparent conductivity (orange color) along each side of the dam's centerline. Soil compaction and reduced moisture contents may be responsible for the slightly lower apparent conductivity evident along the dam's centerline. Higher values (>30 mS/m) of apparent conductivity are found in the wetter pool area located on the upstream side of the structure.

In the plots of apparent conductivity (Figure 3, lower plots), low and negative values occur in the abutment areas. The abutments are underlain by resistive sandstone and have values of apparent conductivity less than 0 mS/m. In these plots, areas of blue are presumed to represent areas with thin soils that are underlain by sandstone at relatively shallow depths. In the lower plots of Figure 3, as deeper depths and greater columns of bedrock are profiled (lower frequency), the areas of negative conductivities (blue and purple colors) expand along each abutment.

In each of the apparent conductivity plots, a sequence of color bands extends outwards from the more conductive embankment materials to the more resistive earthen materials of the abutments. Because of the banded color patterns along the abutments, one could easily, but falsely, conceive pathways where a breach and flow have occurred. Such interpretations are not acceptable. No clear evidence supporting these pathways is apparent in the data.

In each of the apparent conductivity plots, three point anomalies (P) are visible along the lower portion of the upstream embankment. These are the same anomalies that were identified in the plots of the in-phase data. In addition, two point anomalies (A) are evident in the plot of apparent conductivity data collected at 9810 Hz. The anomaly that occurs along the left abutment is also apparent in the plots of apparent conductivity data collected at 3030 and 6150 Hz. These anomalies occur at the same locations as the two anomalies (A) evident in the in-phase data. They are presumed to be related to the foundation drainage.

In Figure 3, in the plots of apparent conductivity data, the spatial patterns principally reflect the embankment materials and the underlying lithology. No unambiguous evidence of pathways, where a breach and flow have occurred, is identifiable in these plots. This suggests that the breach and flow pathway are too small or lacks sufficient contrast to be detected with EMI.

Figure 4 is a two-dimensional color image of the apparent conductivity data collected at 3030 Hz superposed on a three-dimensional surface net of the survey site. This figure was prepared merely to provide an alternative

perspective into the spatial patterns of apparent conductivity measured at the site.

A second survey of the site was conducted with the GEM300 sensor operated manually in the station mode. Apparent conductivity measurements collected in the station mode at each of the 108 survey points are shown in Figure 5. Measurements were made at frequencies of 3030, 6150, 9810, and 14790 Hz. In Figure 5, data collected in the horizontal and vertical dipole orientations are shown in the left-hand and right-hand columns, respectively. The orientation (either vertical or horizontal) of the transmitter and receiver coil axis with respect to the ground surface affects the response from materials at different depths. In the horizontal dipole orientation, the instrument is more sensitive to near surface materials. In the vertical dipole orientation, the instrument is more sensitive to deeper materials.

In Figure 5, the image maps use different colors to represent the data. In each plot, the color interval is 1 mS/m. The locations of the flagged, survey points are shown in the upper left-hand plot (3030 Hz, horizontal dipole orientation). The frequency at which data were collected is shown to the left of each horizontal pair of plots. The depths of penetration and observation are assumed to increase as the frequency decreases (in Figure 5, from bottom to top).

Similar spatial patterns are evident in each of the plots shown in Figure 5. For each frequency, in the embankment and pool areas, conductivity increases with increased depth (vertical dipole measurements are greater than horizontal dipole measurements). However, the use of different frequencies reveals that this relationship does not hold for all profiled depths (depths increase with decreasing frequency). Within the embankment, apparent conductivity measured at 6150 Hz is generally higher than apparent conductivity measured at 9810 and 3030 Hz. Along the abutments, apparent conductivity decreases with decreasing frequency and increasing observation depths. However, in the right abutment, measurements obtained in the shallower sensing horizontal dipole orientation are generally lower than those obtained in the deeper-sensing vertical dipole orientation. Differences in the underlying lithologies may explain these relationships.

The spatial patterns apparent in Figure 5 are similar to those in the plots of apparent conductivity shown in Figure 3. These patterns reflect the embankment materials and underlying lithology. No evidence of pathways, where a breach and flow have occurred, is identifiable in these plots.

**Summary:**

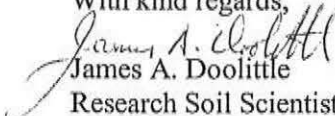
Results from the EMI survey revealed no evidence of a major breach or conduit for water movement along the left abutment. In all probability, the conduit(s) is either too small and/or lacks sufficient contrast with the surrounding earthen materials to be detected with EMI. It is recommended that persons more knowledgeable of the site review these plots.

Plots of apparent conductivity principally reflect the properties of the embankment materials and underlying lithology. The in-phase data appear to provide information concerning the location of buried structural and cultural features.

On request, all files and plots will be forwarded to your office. Please specify format for Surfer files (AutoCAD DXF, Tagged Image, Window Bitmap, JPEG Compressed Bitmap).

It was my pleasure to work once again in Wisconsin and with members of your fine staff.

With kind regards,

  
James A. Doolittle  
Research Soil Scientist

## cc:

R. Ahrens, Director, USDA-NRCS, National Soil Survey Center, Federal Building, Room 152, 100 Centennial Mall North, Lincoln, NE 68508-3866

Barbara Lensch, Geologist, USDA-NRCS, 6515 Watts Road, Suite 200, Madison, Wisconsin 53719-2726

C. Olson, National Leader, Soil Investigation Staff, USDA-NRCS, National Soil Survey Center, Federal Building, Room 152, 100 Centennial Mall North, Lincoln, NE 68508-3866

J. Ramsden, State Conservation Engineer, USDA-NRCS, 6515 Watts Road, Suite 200, Madison, Wisconsin 53719-2726

H. Smith, Director of Soils Survey Division, USDA-NRCS, Room 4250 South Building, 14th & Independence Ave. SW, Washington, DC 20250

**References:**

- Butler, D. K., J. L. Llopi, and C. M. Deaver. 1989. Comprehensive geophysical investigation of an existing dam foundation. *Geophysics: The Leading Edge of Exploration*. 8(8): 10-18.
- Greenhouse, J. P., and D. D. Slaine. 1983. The use of reconnaissance electromagnetic methods to map contaminant migration. *Ground Water Monitoring Review* 3(2): 47-59.
- Kachanoski, R. G., E. G. Gregorich, and I. J. Van Wesenbeeck. 1988. Estimating spatial variations of soil water content using noncontacting electromagnetic inductive methods. *Can. J. Soil Sci.* 68:715-722.
- McNeill, J. D. 1980. Electrical Conductivity of soils and rocks. Technical Note TN-5. Geonics Ltd., Mississauga, Ontario. p. 22.
- McNeill, J. D. 1991. Advance in electromagnetic methods for groundwater studies. *Geoexplorations* 27:65-80.
- McNeill, J. D. 1996. Why doesn't Geonics Limited build a multifrequency EM31 or EM38 meter? Technical Note TN-30. Geonics Limited, Mississauga, Ontario. 5 p.
- Olayinka, A. I. 1990. Electromagnetic profiling for groundwater in Precambrian basement complex areas of Nigeria. *Nordic Hydrology* 21:205-216.
- Rhoades, J. D., P. A. Raats, and R. J. Prather. 1976. Effects of liquid-phase electrical conductivity, water content, and surface conductivity on bulk soil electrical conductivity. *Soil Sci. Soc. Am. J.* 40:651-655.
- Roy, A. and A. Apparao. 1971. Depth of investigation in direct current methods. *Geophysics* 36:943-959.
- Won, I. J., Dean A. Keiswetter, George R. A. Fields, and Lynn C. Sutton. 1996. GEM-2: A new multifrequency electromagnetic sensor. *Journal of Environmental & Engineering Geophysics* 1:129-137.

# TOPOGRAPHIC MAP OF SITE 24 BAD AXE WATERSHED

Contour Interval = 2 ft

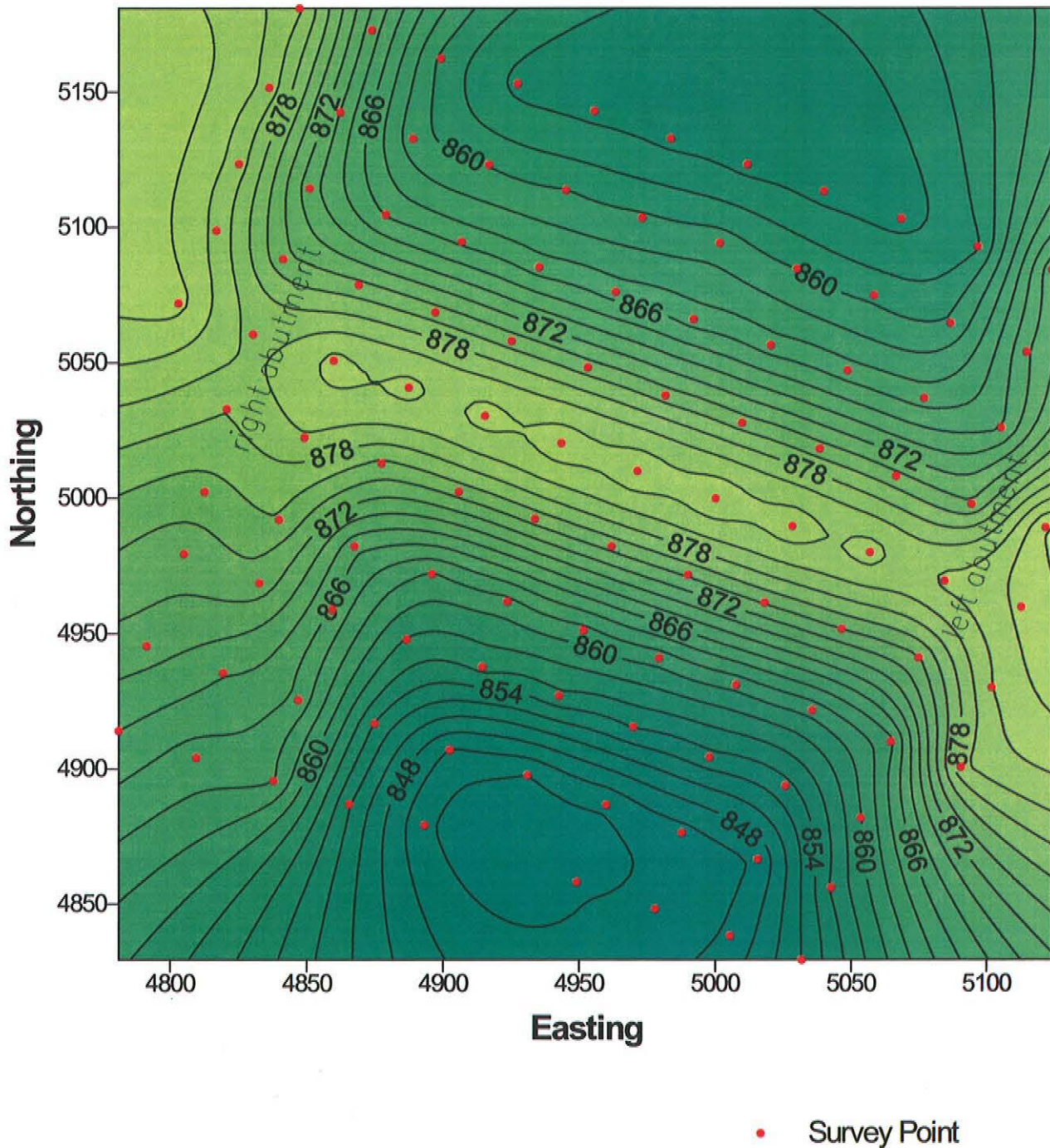
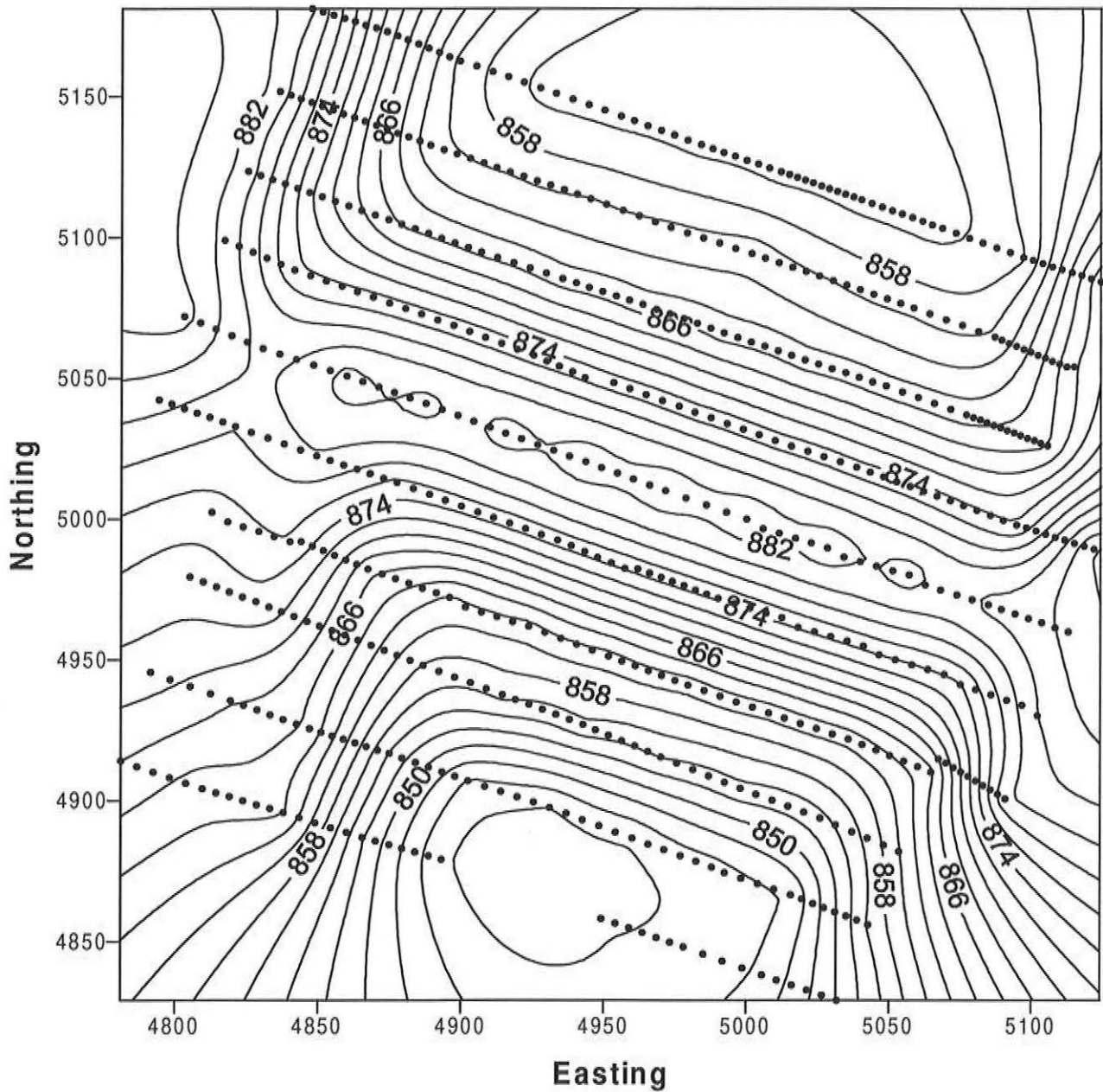


Figure 1

# LOCATION OF OBSERVATION POINTS SITE 24, BAD AXE WATERSHED

GEM300 SENSOR  
CONTINUOUS MODE



• Observation Point

Figure 2

# EMI SURVEY OF SITE 24, BAD AXE WATERSHED GEM300 SENSOR - VERTICAL DIPOLE ORIENTATION

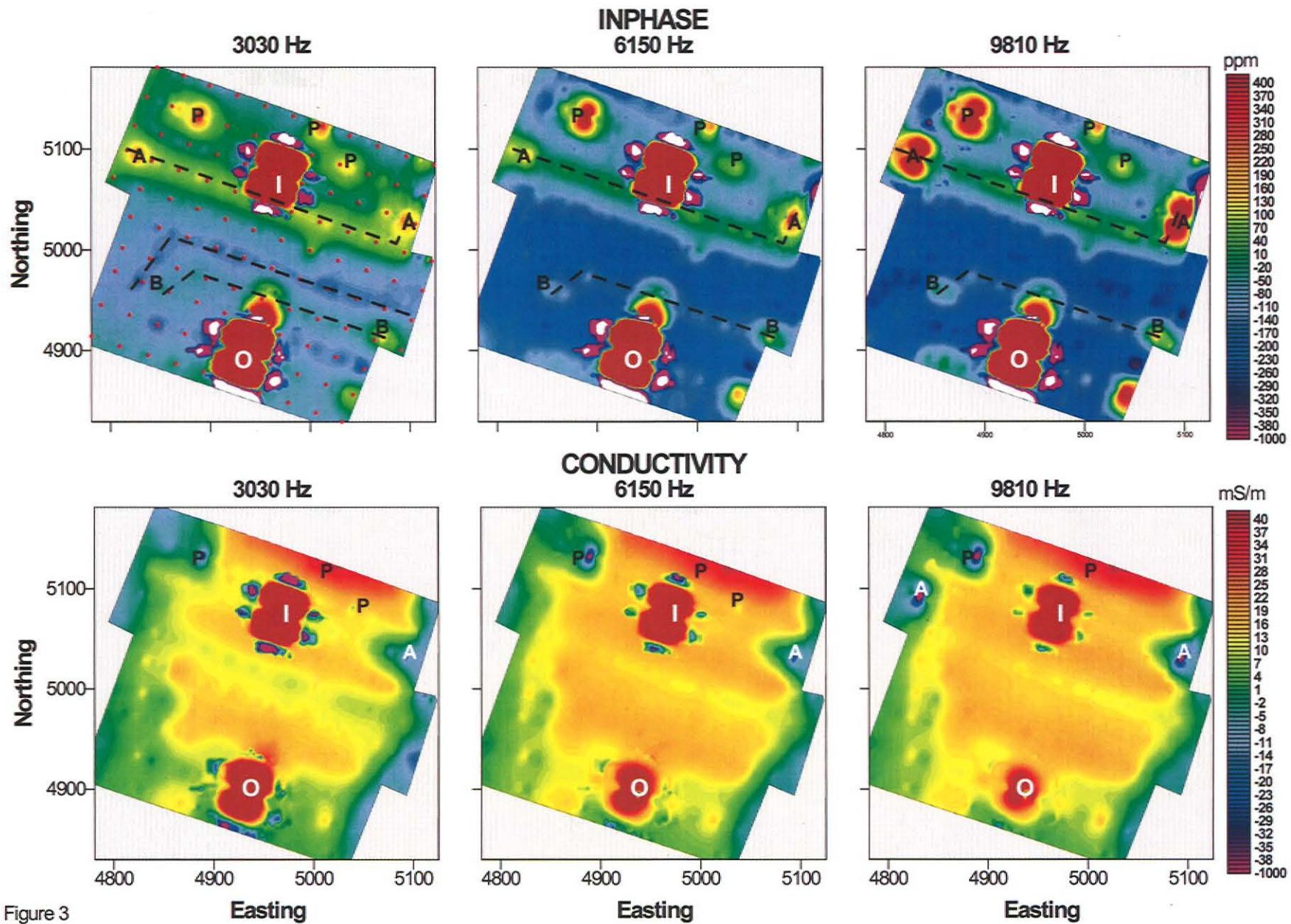


Figure 3

# EMI SURVEY OF SITE 24, BAD AXE WATERSHED GEM300 SENSOR 3030 Hz - CONDUCTIVITY

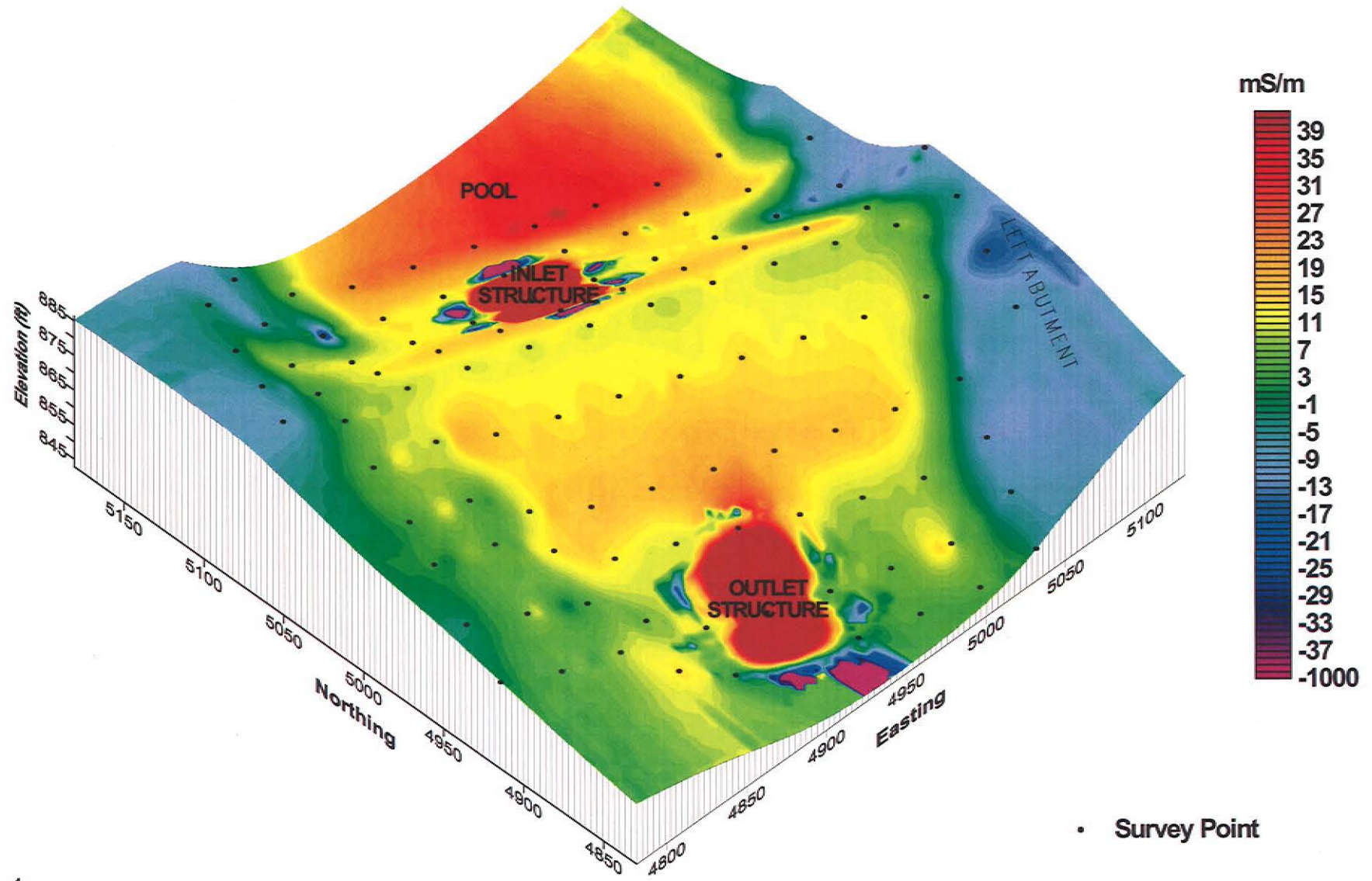


Figure 4

# EMI SURVEY OF SITE 24, BAD AXE WATERSHED GEM300 SENSOR

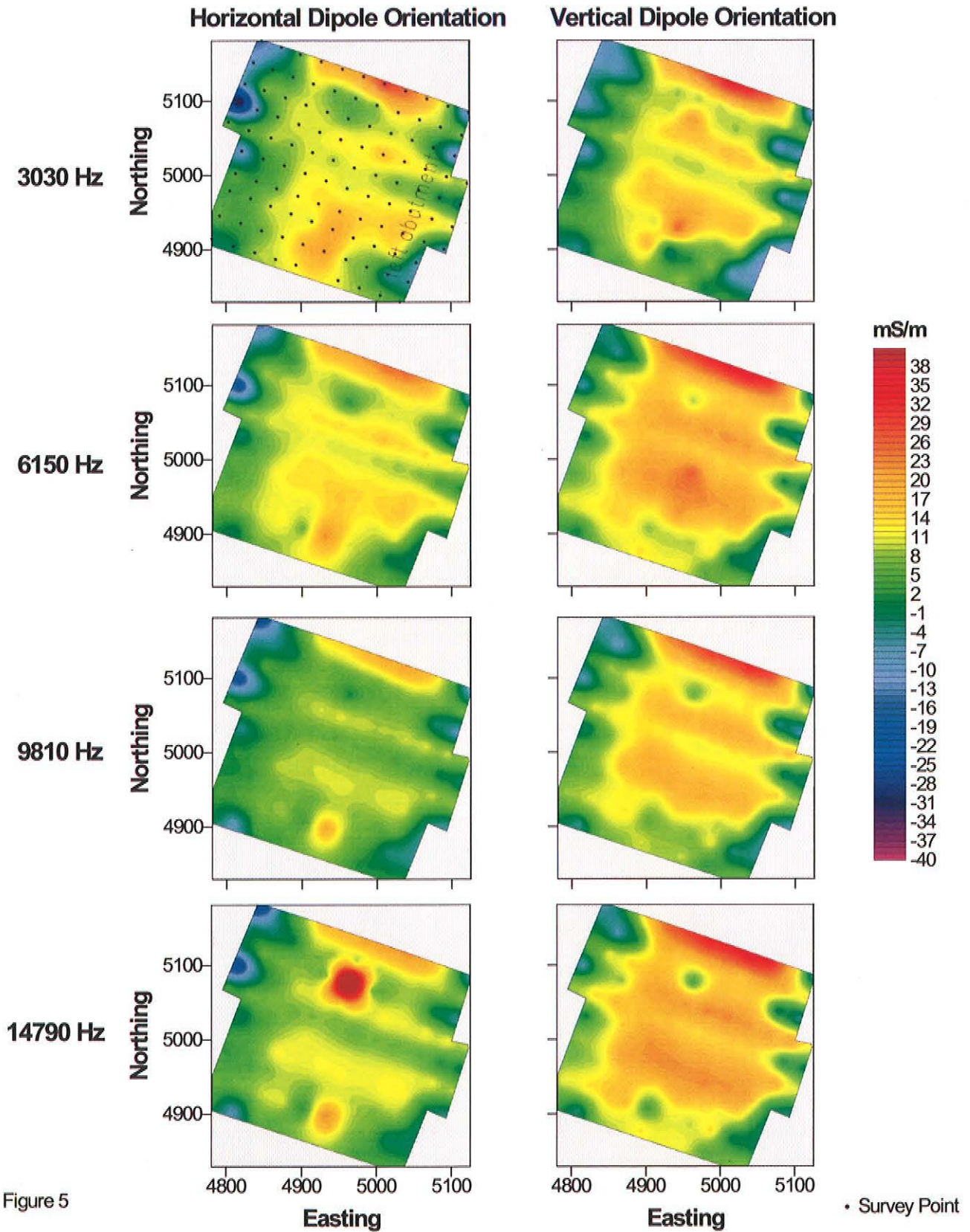


Figure 5